Raman mapping of the microdeformed zone produced by Vickers and Knoop microindentation techniques in poly(vinylidene fluoride)

T. Jawhari, J. C. Merino, J. C. Rodriguez-Cabello and J. M. Pastor*
Física de la Materia Condensada, Facultad de Ciencias, Universidad de Valladolid, Valladolid 47011, Spain
(Received 7 February 1992; revised 12 June 1992)

Raman microspectroscopy was used to follow the crystalline phase transformation produced when Knoop and Vickers microindentations are made in poly(vinylidene fluoride). An evolution of the degree of crystalline phase transformation was observed along the microindentations which can be schematized into three regions. A high gradient in the degree of crystalline transformation was detected near the centre of the indentation, whereas Raman microanalysis of the region near the edges of the impression did not indicate a significant variation in the crystalline phase modification. An explanation for these observations is proposed.

(Keywords: microindentation; Vickers; Knoop; Raman mapping; microdeformation; poly(vinylidene fluoride))

INTRODUCTION

During the last decade, developments in the Raman microspectroscopy technique have opened new perspectives in the field of vibrational spectroscopy owing to its very high spatial resolution (of the order of micrometres) and the fact that the microregion under study can be analysed without any sample preparation, thus eliminating the risk of modifying its structure. In this work we illustrate how the Raman microspectroscopy technique can be applied in the field of polymer science by analysing the microdeformed region produced when a Vickers or Knoop indentation is made in a semi-crystalline polymer.

Microhardness reports on polymers have recently started to appear in the literature[1–7]. The microhardness test, which consists of producing a microindentation at the surface of the material to be studied and measuring the size of the impression, has provided valuable information on the resistance to deformation. The mechanisms of the process of microindentation are still little known, principally due to the absence of direct analysis of the microdeformed region. Few theoretical models[8,9] have been proposed to explain the mechanisms of deformation during the process of microindentation. Some of these theoretical models were found to fit well the experimental data obtained for some types of material, e.g. rigid-plastic compounds, but not for others such as elastic-plastic materials. In the case of polymers the situation is even more complex due to the different properties (e.g. glassy, viscoelastic behaviour) that can be exhibited by a polymeric material and which are highly dependent on temperature. Another difficulty with polymers is that the microhardness value is also affected by the degree of crystallinity, lamellar thickness, molecular weight, degree of branching, thermal history of the sample, etc. Previous works attempted to correlate the microhardness value to some of these parameters[4,10–13].

It is known[14] that the deformation produced in polymers by either compressive or tensile force may result in a crystalline phase transformation; for example, this is the case for polymeric materials such as poly(3,3-dimethyl oxetane) (PDMO)[15] and poly(vinylidene fluoride) (PVF_2)[16]. In previous work[17,18] we have shown that Raman spectroscopy can be a very useful technique to study and follow the crystalline variation due to compressive deformation. These results, which were obtained on PDMO[17] and PVF_2[18], clearly indicated that the degree of crystalline transformation varies gradually along the deformed zone. The purpose of this work is to complete the initial studies carried out on the microindentation process in polymers by analysing the results obtained with two different indenter geometries, i.e. Vickers and Knoop indenters. The profile of crystalline transformation inside the two different microindentations was obtained by realizing and analysing the microRaman mapping of the deformed polymer zone.

EXPERIMENTAL

The poly(vinylidene fluoride) sample utilized was the commercial material PVDF SOLEF-1012, provided by Solvay & Cie. For the microhardness experiment, a 5 mm thick polymer plate was produced by hot-pressing PVF_2 pellets at 210°C and then cooling at room temperature.

Polymer deformation was produced using two

*To whom correspondence should be addressed

0032-3861/93/081613-07
© 1993 Butterworth-Heinemann Ltd.

microindenters of different geometry. The first series of microindentations was produced as per the typical Vickers microhardness testing method, i.e. with a square pyramidal diamond indenter with an apical angle of 136° (between non-adjacent faces of the pyramid). The other microindentations were obtained using the Knoop test, usually employed to determine anisotropic properties, in which indentations are made with an asymmetrical, rhombic-based pyramidal diamond indenter with angles of 172° and 130° between opposite edges and where the major diagonal is about seven times longer than the minor diagonal. The microindenter instrument was combined with an optical universal Zeiss microscope which allowed visualization and measurement of the microindentation size. The indentations were made at room temperature and the loads were applied for 1 min.

The Raman instrument employed, a Dilor XY spectrometer, comprised a subtractive dispersion double monochromator coupled to a spectrograph combined with multichannel detection (512 intensified diodes). The Raman instrument was coupled to a standard Olympus microscope and the collection optics system used the backscattering configuration. The excitation source was provided by a Spectra Physics argon-ion laser (model 2020/5w), emitting radiation at 514.5 nm. The laser power at the sample position was of the order of 10 mW and the spectral bandpass was fixed at 150 μm. A time acquisition of 2 s was used and the number of scans was 50. The microRaman spectra were recorded with an objective lens of $\times 100$ magnification, which allowed collection of spectra with a spatial resolution of 2 μm[17]. In the case of the Vickers indentation spectra were recorded symmetrically at intervals of 5 μm for the zone close to the centre of the indentation, where the maximum degree of crystalline transformation was observed. For the Knoop indentation the spectra were recorded at different intervals, depending on the direction along the impression due to the asymmetrical rhombic-based pyramidal geometry of the indenter. The position of the sample under the microscope was adjusted manually, the error in the position data being about ± 1 μm. For these experiments, the actual spatial resolution of the mapped data was determined, at best, by the sampling interval, i.e. 5–10 μm. The different positions where Raman spectra were collected are illustrated in *Figures 1a* and *1b*, respectively, for the Vickers and Knoop microindentations. In both cases spectra were collected along one face of the impression only, assuming that the distribution of tensions is symmetrical with respect to the two diagonals of the indentation.

The optical micrographs presented in this work were obtained with a Nomarski differential interference contrast microscope, which provides a sharply defined, relief-like image.

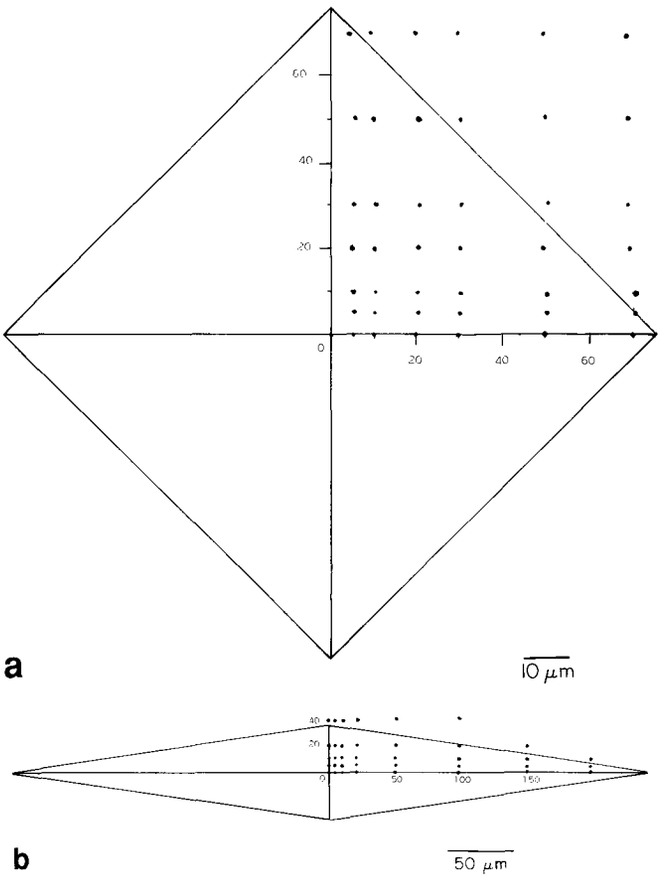

Figure 1 Graphic representation of the different positions where Raman spectra were recorded along (a) the Vickers microindentation and (b) the Knoop microindentation

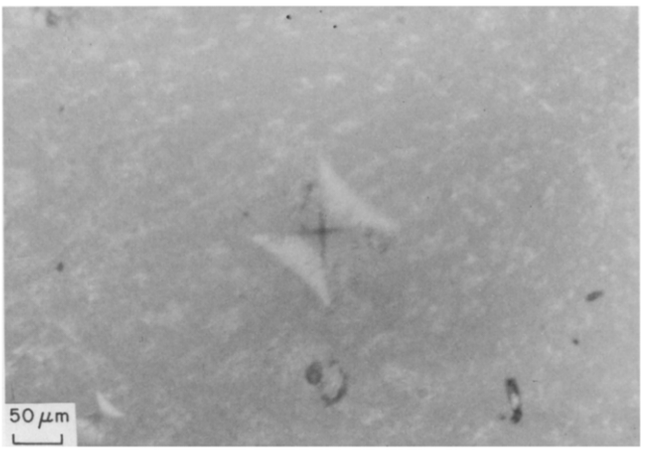

Figure 2 Photograph of the Vickers microindentation obtained with a load of 2 N and taken with a microscope objective of $\times 20$

RESULTS

Microindentations were produced in PVF_2 using the Vickers and Knoop indenters under a load of 2 N; photographs of these two microindentations are presented in *Figures 2* and *3*. The dimension of the diagonals is ~ 150 μm for the Vickers indentation and 480 μm and 70 μm, respectively, for the major and minor diagonals of the Knoop impression. Careful observation of *Figure 3* reveals the presence of two distinct regions; a dark region (labelled zone A) in the centre of the Knoop microindentation having a minor diagonal length of 40 μm surrounded by a second, lighter zone (zone B), which extends up to 70 μm. This last value is approximately equal to one-seventh of the major diagonal, which agrees well with the ratio of the two diagonals of the indenter. As will be explained below, the variation in tonality can be attributed to the different types of deformation process that predominate in each region. Similarly, from the micrograph of the Vickers microindentation, a slight difference in tonality can be discerned between the central region of the indentation and the surrounding zone. Further, the micrograph of

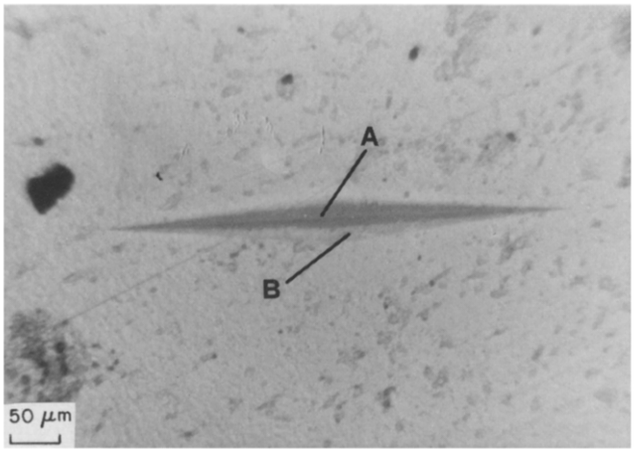

Figure 3 Photograph of the Knoop microindentation obtained with a load of 2 N and taken with a microscope objective of × 20, with the different zones indicated as A and B

Figure 2 displays an impression with the curved edges characteristic of indentation in polymeric materials that show a high degree of recovery as the indenter is retrieved[3,19]. As can also be observed, the recovery is greater along the direction of maximum gradient in depth – i.e. along the direction at 45° if we consider that the two diagonals of the microindentation constitute the two axes of a Cartesian coordinate system – than along the diagonals.

The crystal transformation in PVF_2 from form II(α) to form I(β) has been studied by analysing the changes occurring in the Raman spectrum. The two bands present in the Raman spectrum of PVF_2 at 799 and 840 cm^{-1} have been assigned to the non-planar (TGTG') conformation (form II(α)) and to the planar zigzag (TTTT) conformation (form I(β)), respectively[20–23]. Since we have shown in a previous study[18] that the application of a pressure or a tension on PVF_2 produces a gradual phase transformation from the structure II(α) to structure I(β) that depends on the degree of pressure or tension submitted to the sample, the ratio $R = I_{840\,cm^{-1}}/(I_{840\,cm^{-1}} + I_{799\,cm^{-1}})$ can be used to obtain a relative value of the degree of phase I(β) in the sample studied. (The ratio R was determined by measuring the peak height of the two Raman bands without deconvolution of the data.)

The microRaman spectra were recorded, between 650 and 950 cm^{-1} approximately, at the positions along the Vickers and Knoop indentation surfaces indicated in *Figures 1a* and *1b*, respectively. The Raman spectra of PVF_2 recorded in the centre of and outside the Knoop microindentation are given as an example in *Figure 4*. The ratio R was calculated for each position and then plotted in a three-dimensional map with the aid of a graphic program that gives the best interpolation between each point (see *Figures 5* and *6*). In order to estimate the experimental error when calculating the value of R, a series of six spectra were recorded at 10 μm intervals outside the Knoop impression. The average value and standard deviation for this series of six measurements are 0.210 and 0.008 respectively, which gives an error on the measurement of about $\pm 4\%$. This experimental error is thought to be principally due to structural inhomogeneities in the sample and, although it limits the accuracy of the data, it is considered low enough to indicate the approximate trend of the crystalline form variation within the microindentation.

The variation in the ratio of the crystalline form along the microindentation can be better followed by presenting contour lines of identical degree of crystalline phase transformation. In *Figures 7* and *8* the contour lines are plotted for each projected indentation with an interval contour line of 0.01.

Figures 5 and *6* clearly show that in both microindentations the crystalline transformation varies along the Knoop and Vickers impressions, confirming initial results[17,18] that the distribution of pressure is not constant along the indentation but rather increases as the centre of the impression is approached. Further, it can be observed that the crystalline form modification along both diagonals of the Vickers indentation is equivalent whereas the Knoop indentation shows a large anisotropic profile.

From the contour lines plotted in *Figure 7* it can be observed that the profile of the crystalline transformation appears to be circular in a region of ~ 20 μm diameter around the centre of the Vickers indentation, i.e. over about 13% of the whole indentation. Outside this region the circular contour becomes distorted, especially near the diagonals of the impression. In the case of the Knoop

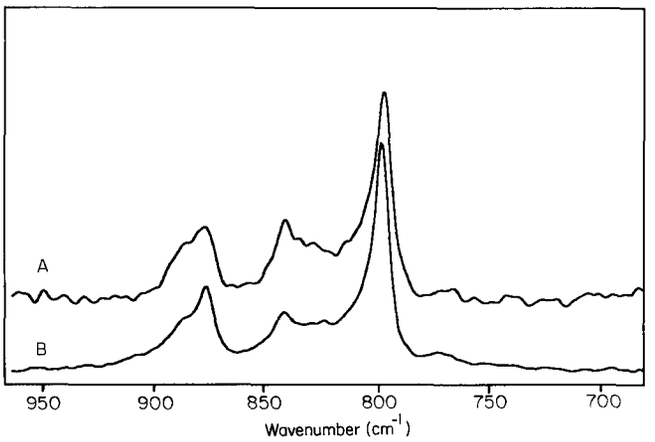

Figure 4 Raman spectra of PVF_2 recorded in the centre of the Knoop microindentation (A) and outside the deformed zone (B)

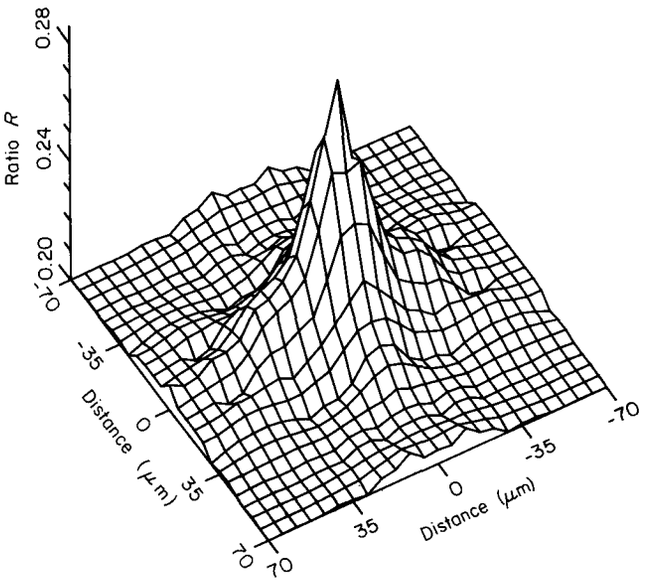

Figure 5 Three-dimensional map showing the variation of the ratio R along the Vickers indentation

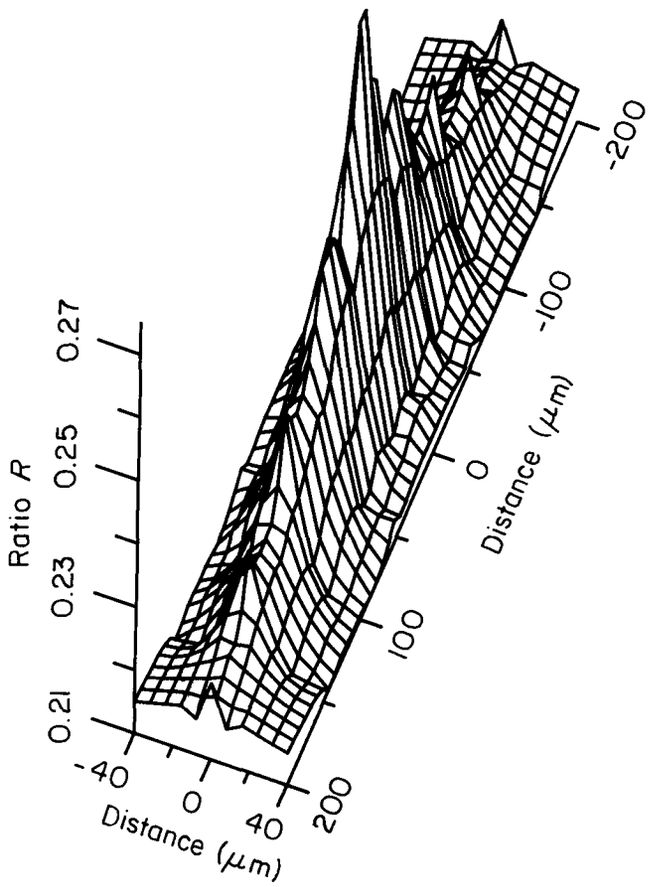

Figure 6 Three-dimensional map showing the variation of the ratio R along the Knoop indentation

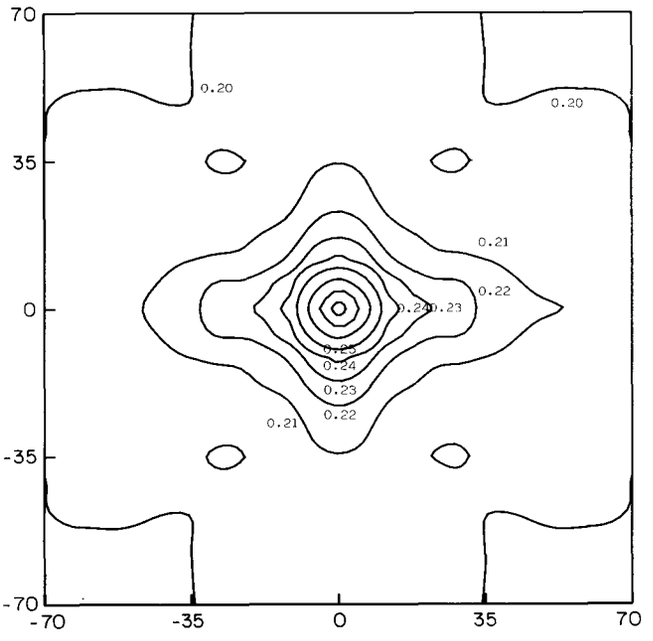

Figure 7 Contour lines of the ratio R plotted in the projected Vickers indentation with an interval contour line of 0.01

indentation the anisotropic profile of the contours seems to increase with increasing distance from the centre. It should here be recalled that data were collected from only one quadrant and that the observed geometry in *Figures 7* and *8* is due to reflection of the data over the whole indent region.

The variations of R as a function of distance from the centre of the Vickers indentation, along both the diagonal and the line of maximum gradient in depth at 45°, is presented in *Figure 9a*. In this figure, R seems to decrease more rapidly along the line of maximum gradient in depth than along the diagonal for distances greater than $\sim 10\ \mu m$ from the centre of the indentation.

Figure 10a is a plot of R *versus* the distance from the centre of the Knoop indentation along its two diagonals. This figure clearly indicates the anisotropy in the degree of crystalline transformation that occurs in the Knoop indentation.

Now, instead of plotting R *versus* the distance from the centre, it is interesting to examine how the crystalline form modification varies with depth along the indentation. Plots of R *versus* the variation of depth along the diagonal and the direction at 45° for the Vickers indentation, and along the two diagonals of the Knoop indentation are given in *Figures 9b* and *10b*, respectively. Here, the depth value is obtained from the position corresponding to the contact surface of the material with the loaded indenter, i.e. the depth value is calculated from the measurement of the diagonal. From *Figures 9b* and *10b* it can be observed, more clearly in the case of the Knoop experiment, that the plots are approximately similar for the two different directions in each indentation. Thus, the variation in the crystalline transformation appears to be independent of direction when plotted against the variation of depth along the indentation. As will be discussed later in the text, this suggests that the depth is an important parameter of the indentation process affecting the crystalline phase transformation.

In the Vickers indentation most of the crystalline phase transformation occurs near the centre of the impression; for example, 70% of the crystalline form transition is produced in the central region corresponding to approximately 20% of the total surface of the indentation.

Similarly, in the case of the Knoop indentation, most of the crystalline variation along both the major and minor diagonals occurs within a distance smaller than the total diagonal length; for instance, about 90% of the total crystalline transformation is produced in 65% of the major diagonal length and the whole crystalline transformation along the minor diagonal takes place in a region of about 60% of the total diagonal length.

DISCUSSION

From the analysis of the Raman mapping of the Vickers and Knoop microindentations, three different zones can be distinguished:

(i) a region in the centre of the impression (of circular profile $\sim 20\ \mu m$ in diameter in the case of the Vickers indentation) which corresponds to the highest gradient of crystalline phase transformation in the impression;

(ii) a second region surrounding the central zone which shows a much lower gradient of phase transition than the central region;

(iii) a third region which presents very little crystalline form variation. This zone corresponds to region B indicated on the micrograph of the Knoop microindentation in *Figure 3*.

The presence of these three zones may be understood by considering the different models that have been proposed to describe the process of microindentation by

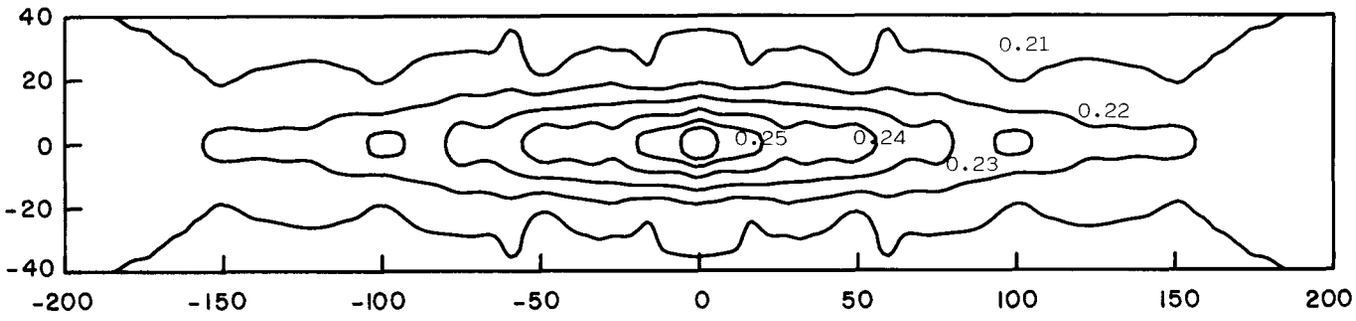

Figure 8 Contour lines of the ratio R plotted in the projected Knoop indentation with an interval contour line of 0.01

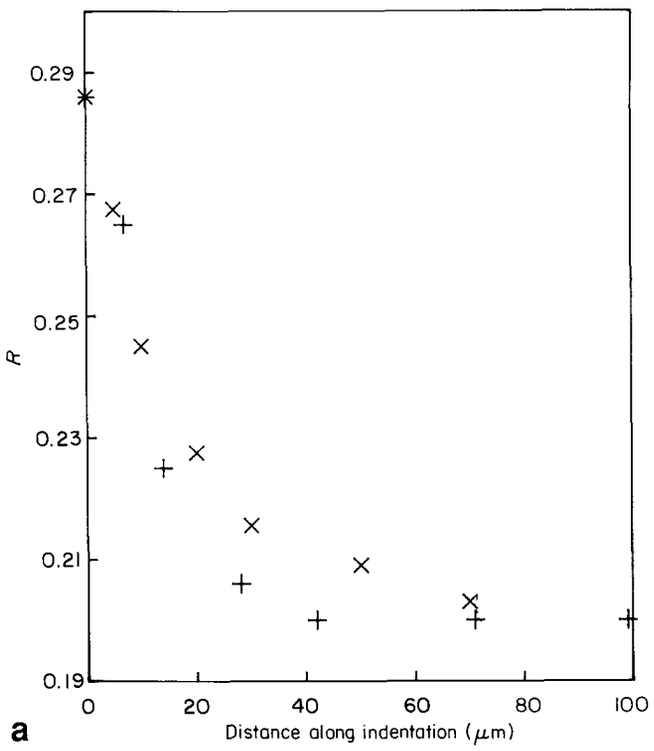

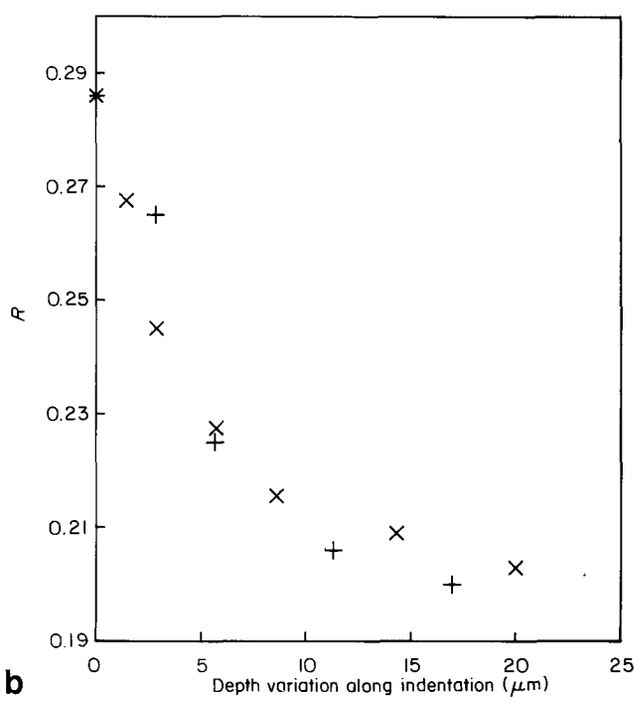

Figure 9 Plot of R *versus* (a) distance from the centre and (b) depth variation (the origin being taken at the centre of the indentation) of the Vickers indentation: ×, along the diagonal; +, along the line of maximum gradient in depth (*Figure 9a*) or the direction at 45° (*Figure 9b*)

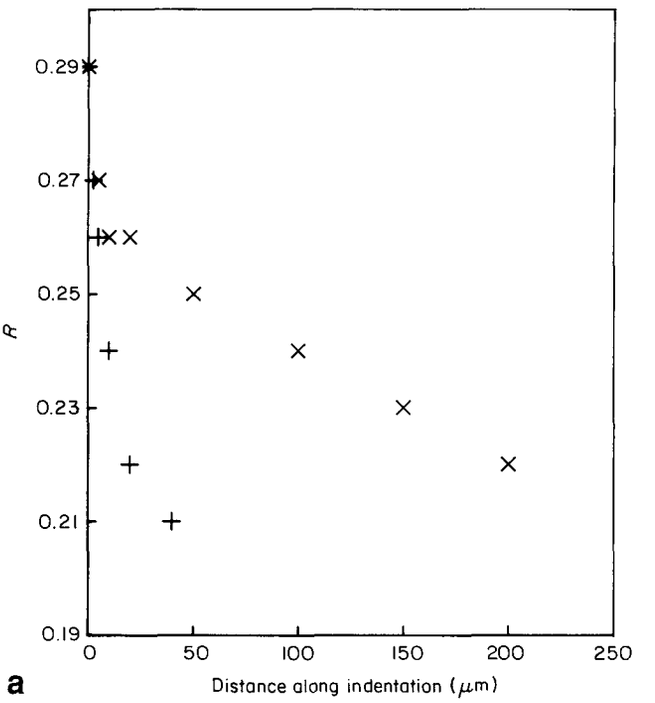

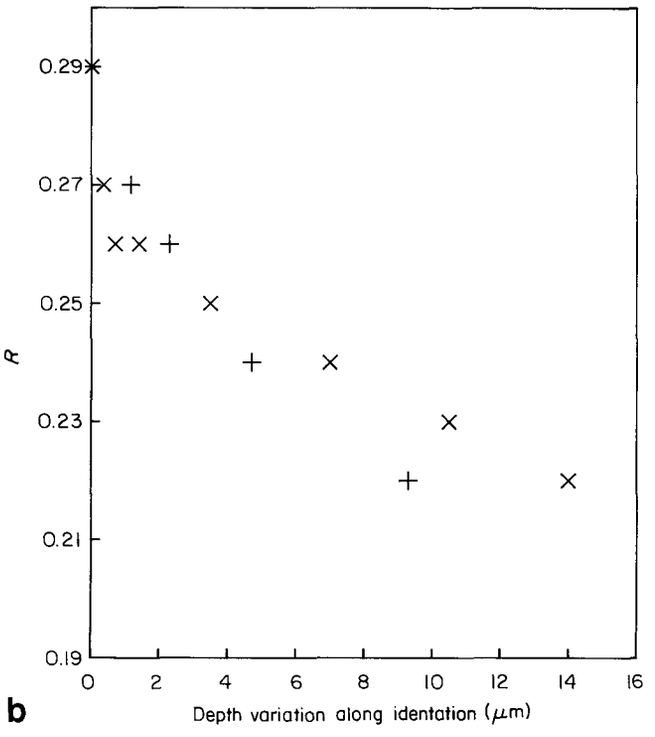

Figure 10 Plot of R *versus* (a) distance from the centre and (b) depth variation (the origin being taken at the centre of the indentation) of the Knoop indentation: ×, along the major diagonal; +, along the minor diagonal

blunt indenters. The results presented in *Figures 9b* and *10b*, in which the degree of crystalline transformation is similar for different directions along the microindentation and for different indenter geometries when plotted against the variation in depth, suggest that in the second zone the process of deformation occurs principally through a radial compression mechanism. Such a result is in good agreement with the model proposed by Mulhearn[24] to describe the process of microindentation by a blunt indenter in metals. In this model, the deformation of the sample occurs by radial compression of hemispherical shells centred at the point of first contact, with the magnitude of the strains diminishing as the elastoplastic boundary is approached. This could explain why the distribution in the crystalline phase transformation decreases along the microindentation as the distance from the centre increases and approaches the edge of the indentation. However, such a model fails to describe the large gradient in crystalline transformation that was observed in the central zone of the microindentation near the tip of the indenter. This central zone occurs in the region close to the point of discontinuity, i.e. the tip of the microindenter. A similar, but less pronounced effect is also expected near the intersections of the pyramid facets, i.e. the diagonals of indenter.

Before interpreting these results further it is convenient to describe the mechanisms that produce crystalline phase transformation in a polymer submitted to pressure. The consequence of applying pressure to a sample is to generate flow in the material and, since polymers are formed of chains which are more or less entangled, deformation in the material due to the process of flow in the bulk produces tensions along the polymer chains which are more or less effective, depending on the degree of entanglement and the type of deformation imposed on the material. For example, it is expected that propagation of the tensions to the polymer chains would be more effective during uniaxial deformation flow (e.g. uniaxial drawing) than in the case of compressive deformation. This was effectively confirmed by results obtained in this laboratory, where Raman spectra of PVF_2 samples deformed under uniaxial forces and compressive forces were analysed and compared, similarly to previous work on PDMO[15]; the results indicated that the degree of crystalline transformation is much higher in the case of the drawing experiments than in the compressive deformation. Thus it follows that the resulting tensions along the polymer chains produce the crystalline transformation observed in semicrystalline polymers such as PDMO and PVF_2.

As commented previously, the dominant deformation process occurring in the second zone of the microindentation arises through radial compression of the material. Therefore, the degree of crystalline transformation depends on the displacement in depth of the material below the indenter. Near the tip of the indenter and to a lesser degree along the diagonals, there is another additional effect that makes more effective the propagation of tension to the polymer chains – the sharp discontinuity in the geometry of the indenter. In this region, the material will be involved in strain fields of different directions which will further increase the degree of tension along the polymer chains. This will therefore result in an increase of the crystalline phase transformation near the tip of the indenter and thus explains the high degree of crystalline transformation observed in the central region.

Finally, in the third region of the microindentation, no significant variation in crystalline phase transformation could be detected. This result could be explained by the elastoplastic model proposed by Loubet *et al.*[25]. In this region the contribution of elastic deformation is greater than in the first and second regions, mainly due to the deflection of the material surface that usually occurs just outside the zone in contact with the indenter during the indentation of polymeric materials. Elastic deformation appears to be the dominant process in this third region and as a result little crystalline transformation takes place. Our results on crystalline phase transformation in PVF_2 are thus in good agreement with the information given by the optical micrograph of *Figure 3*, in which the different tonalities detected by the Nomarski differential interference contrast microscope show a clear variation in the slope of the impression due to the recovery that mainly affects the region near the edges of the indentation (zone B in *Figure 3*).

CONCLUSIONS

In conclusion, the Raman mapping study of Vickers and Knoop microindentations in PVF_2 shows the existence of three zones which appear to depend on the elastoplastic behaviour of the material and on the type of deformation to which the material is subjected (principally determined by the geometry of the indenter).

Near the centre of the indentation, the high degree of crystalline transformation is probably due to the sharp discontinuity in the geometry of the indenter. The material is involved in strain fields of different directions, thus increasing the tensions along the polymer chains.

In the second zone the dominant deformation process takes place through radial compression of the material, with the crystalline variation diminishing as the displacement in depth of the material surface below the indenter decreases.

Finally, in the third region of the impression, near the edges of the indenter, elastic deformation appears to be the main mechanism of deformation. As a result, little crystalline phase transformation was detected in this region.

ACKNOWLEDGEMENTS

This work has been carried out with the support of the CICYT (MAT90-0914) and the Junta de Castilla y León (1605/90).

REFERENCES

1 Crawford, R. J. *Polym. Test.* 1982, **3**, 37
2 Balta-Calleja, F. J., Martinez-Salazar, J. and Rueda, D. R. 'Encyclopedia of Polymer Science and Engineering' (Eds H. F. Mark, N. M. Bikales, C. G. Overberger and G. Menges) Vol. 7, John Wiley & Sons, New York, 1987, p. 614
3 Howes, V. R. and Wall, P. *J. Appl. Polym. Sci.* 1987, **34**, 1125
4 Pastor, J. M., González, A. and Saja, J. A. *J. Appl. Polym. Sci.* 1989, **38**, 2283
5 Gonzalez, C. C., Pereña, J. M., Bello, A., Martin, B., Merino, J. C. and Pastor, J. M. *J. Mater. Sci. Lett.* 1989, **8**, 1418
6 Deslandes, Y. and Alva Rosa, E. *Polym. Commun.* 1990, **31**, 269
7 Balta Calleja, F. J., Santa Cruz, C., Sawatari, C. and Asano, T. *Macromolecules* 1990, **23**, 5352
8 Samuels, L. E. 'Microindentation Techniques in Materials Science and Engineering' (Eds P. J. Blau and B. R. Lawn) ASTM, Philadelphia, 1986, p. 5

9 Tabor, D. 'Microindentation Techniques in Materials Science and Engineering' (Eds P. J. Blau and B. R. Lawn) ASTM, Philadelphia, 1986, p. 129
10 Balta-Calleja, F. J., Martínez-Salazar, J., Cackovic, H. and Loboda-Cackovik, J. *J. Mater. Sci.* 1981, **16**, 739
11 Balta-Calleja, F. J. *Adv. Polym. Sci.* 1985, **66**, 19
12 Balta-Calleja, F. J. and Kilian, H.-G. *Coll. Polym. Sci.* 1988, **266**, 29
13 Lorenzo, V., Pereña, J. M. and Fatou, J. G. *Angew. Makromol. Chem.* 1989, **172**, 25
14 Tashiro, K. and Tadakoro, H. 'Encyclopedia of Polymer Science and Engineering' (Eds H. F. Mark, N. M. Bikales, C. G. Overberger and G. Menges) Suppl. Vol., John Wiley & Sons, New York, 1989, p. 213
15 Merino, J. C., Pastor, J. M., Saja, J. A. and Christen, D. *J. Mol. Struct.* 1986, **143**, 183
16 Tashiro, K. and Kobayashi, M. *Phase Transitions* 1989, **18**, 213
17 Jawhari, T., Merino, J. C. and Pastor, J. M. *J. Mater. Sci.* 1991, **27**, 2231
18 Jawhari, T., Merino, J. C. and Pastor, J. M. *J. Mater. Sci.* 1992, **27**, 2237
19 Muller, K. 'The Science of Hardness Testing and Its Research Applications' (Eds J. H. Westbrook and H. Conrad) ASM, Ohio, 1973, p. 291
20 Boerio, F. G. and Koenig, J. L. *J. Polym. Sci., Part A*-2 1969, **7**, 1489
21 Boerio, F. G. and Koenig, J. L. *J. Polym. Sci., Part A*-2 1969, **9**, 1317
22 Cessac, J. L. and Curro, J. J. *J. Polym. Sci., Polym. Prepr.* 1974, **12**, 695
23 Tashiro, K., Kobayashi, M. and Tadokoro, H. *Macromolecules* 1981, **14**, 1758
24 Mulhearn, T. O. *J. Mech. Phys. Solids* 1959, **7**, 85
25 Loubet, J. L., Georges, J. M. and Meille, G. 'Microindentation Techniques in Materials Science and Engineering' (Eds P. J. Blau and B. R. Lawn) ASTM, Philadelphia, 1986, p. 72